

Doppler Power Spectrum in Channels with von Mises-Fisher Distribution of Scatterers

Kenan Turbic, *Member, IEEE*, Martin Kasparick, and Sławomir Stańczak, *Senior Member, IEEE*

Abstract—This paper presents an analytical analysis of the Doppler spectrum in von Mises-Fisher (vMF) scattering channels. A closed-form expression for the Doppler spectrum is derived and used to investigate the impact of vMF scattering parameters, i.e., the mean direction and the degree of concentration of scatterers. The spectrum is observed to exhibit exponential behavior for the mobile antenna motion parallel to the mean direction of scatterers, while conforming to a Gaussian-like shape for the perpendicular motion. The validity of the obtained results is verified by comparison against the results of Monte Carlo simulations, where an exact match is observed.

Index Terms—Wireless communications, Mobile channel, Statistical model, von Mises-Fisher distribution, Doppler spectrum

I. INTRODUCTION

THE Doppler power spectrum, describing the distribution of received signal power over Doppler frequency shifts, plays a critical role in characterizing fading dynamics in mobile wireless channels [1]. It serves as the foundation for calculating second-order channel statistics, such as the level-crossing rate and average fade duration [2].

Early seminal work on the fading dynamics in mobile channels was presented in [3], where the Doppler spectrum is derived by assuming horizontal propagation and uniform scattering. This work was extended in [4], by considering both the Transmitter (Tx) and Receiver (Rx) in motion. Recognizing the limitations of the uniform scattering assumption, in [5] the authors derive the Doppler spectrum for non-isotropic scattering channels with a von Mises distribution of scatterers.

While these studies assumed 2D propagation, the elevation aspect of 3D propagation was first considered in [6]. This approach was further improved in [7], by incorporating a more realistic scattering distribution in elevation, recognizing the fact that most of the energy propagates horizontally. More recently, in [8] a mixture of von Mises-Fisher (vMF) distributions was proposed as a more suitable model for general non-isotropic 3D scattering. Due to its simplicity and the ability to

approximate arbitrary scattering, this model is widely adopted in the literature. However, the channel statistics under vMF scattering are not fully explored yet, primarily due to the lack of analytically tractable results. While closed-form expressions for correlation characteristics were recently reported in [9], [10], the results for the Doppler power spectrum are not yet available in the literature, to the best of our knowledge.

The existing methods for evaluation of the Doppler spectrum in 3D scattering scenarios either require numerical integration or use spherical waveform expansion framework [11], which yields expressions involving infinite sums of special functions. While applicable to vMF scattering, these methods are computationally intensive and, more importantly, prohibit analytical investigations.

This paper investigates Doppler power spectrum in mobile channels with vMF scattering. As the main contribution of this work, we derive a simple closed-form solution for the Doppler power spectrum directly from the scattering distribution. The obtained result is used to investigate the impact of the scattering parameters, i.e., the mean direction and the degree of concentration of scattering.

The rest of this paper is structured as follows. Section II presents the adopted channel model with the underlying assumptions, while Section III presents derivation of the corresponding Doppler spectrum. The impact of the vMF distribution parameters on the Doppler spectrum is analyzed in Section IV, and the paper is concluded in Section V.

II. CHANNEL MODEL

By considering multipath propagation between the Tx and the Rx, the time-variant frequency-dependent complex transmission coefficient can be written as [12]

$$H(t, f) = \sum_{n=1}^N A_n e^{-j2\pi f \tau_0^n} e^{-j2\pi f f_D^n t} \quad (1)$$

where

t	time;
f	frequency;
N	number of multipath components;
A_n	their amplitudes;
τ_0^n	initial propagation delays;
f_D^n	Doppler frequency shifts.

The multipath components' amplitudes are typically assumed to be approximately constant over local areas, i.e., several tens of wavelengths in size [1]. This means that the

This work was partially supported by the Federal Ministry of Education and Research (BMBF, Germany) in the “Souverän. Digital. Vernetzt.” programme, joint Project 6G-RIC; project identification numbers: 16KISK020K and 16KISK030. It was developed within the scope of COST Action CA20120, Intelligence-Enabling Radio Communications for Seamless Inclusive Interactions (INTERACT).

The authors are with the Wireless Communications and Networks Department, Fraunhofer Institute for Telecommunications, Heinrich Hertz Institute (HHI), Berlin, 10587 Germany (e-mail: kenan.turbic@hhi.fraunhofer.de, martin.kasparick@hhi.fraunhofer.de, slawomir.stanczak@hhi.fraunhofer.de).

Sławomir Stanczak is also with Technische Universität Berlin, Berlin, Germany.

variations in the local average power due to path loss and shadowing can be modeled by an independent stochastic process with much slower dynamics [3], i.e., large-scale fading.

The initial propagation delays, associated with the apparently random propagation path lengths observed at the start of the channel observation period ($t = 0$), result in random phase shifts of multipath components arriving at the Rx. For narrowband communications, these initial phases are typically modeled as uniform random variables, i.e., $\varphi_0^n \sim \mathcal{U}(0, 2\pi)$.

The time-variant phase terms in (1) account for the Doppler effect, associated with changes in the propagation path lengths due to mobile antenna motion. Assuming constant speed, these changes are linear with rates corresponding to Doppler frequency shifts exhibited by each component, i.e.

$$f_D^n = \frac{1}{\lambda} \hat{\mathbf{k}}_n^T \mathbf{v} \quad (2)$$

where

- λ wavelength;
- \mathbf{v} mobile antenna velocity vector;
- $\hat{\mathbf{k}}_n$ Direction of Arrival (DoA)¹ unit vector, i.e.

$$\hat{\mathbf{k}}_n = (\cos \phi_n \cos \psi_n, \sin \phi_n \cos \psi_n, \sin \psi_n)^T \quad (3)$$

- ϕ_n Azimuth Angle of Arrival (AAoA);
- ψ_n Elevation Angle of Arrival (EAoA);
- $(\cdot)^T$ vector transpose operation.

The random DoAs at the arbitrary initial Rx position are represented by the vMF distribution, with the Probability Density Function (PDF) given by [13]

$$p_{\phi\psi}(\phi, \psi) = \frac{\kappa \cos \psi}{4\pi \sinh \kappa} e^{\kappa [\cos \mu_\psi \cos \psi \cos(\phi - \mu_\phi) + \sin \mu_\psi \sin \psi]}, \quad |\phi| \leq \pi, |\psi| \leq \pi/2 \quad (4)$$

where

- μ_ϕ mean AAoA;
- μ_ψ mean EAoA;
- κ spread parameter.

The parameters μ_ϕ and μ_ψ specify the mean direction of the concentrated scattering and κ specifies the degree of angular concentration. For $\kappa = 0$, the vMF distribution becomes uniform over the sphere and the scattering is isotropic, while for $\kappa \rightarrow \infty$ the scattering becomes deterministic with a single scatterer in the direction given by (μ_ϕ, μ_ψ) .

For a large number of multipath components the channel coefficient in (1) exhibits a complex Gaussian distribution, as follows according to the central limit theorem. Assuming that there are no dominant components present, the Rx signal undergoes Rayleigh fading. This case is considered in herein.

It is important to point out that, according to (1), for a single-frequency harmonic signal emitted by the Tx antenna the Rx signal consists of multiple frequency-shifted components. The exhibited frequency shifts are given by (2) and depend on the underlying scattering distribution. The resulting energy distribution across frequency is characterized by the Doppler Power Spectrum Density (PSD).

¹In this work we arbitrarily chose to consider a static Tx and a mobile Rx. However, the same results apply if the roles are reversed.

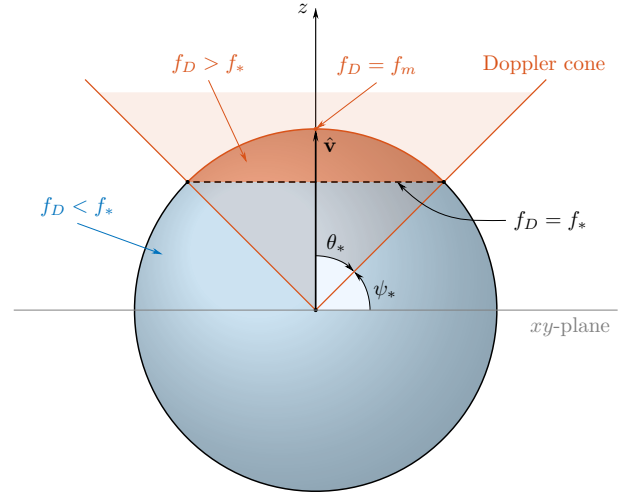


Fig. 1. Doppler cone associated with Doppler shift frequency f_* , for a coordinate system chosen such that the z -axis is aligned with the mobile antenna velocity vector.

III. DOPPLER POWER SPECTRUM

When normalized to unit power, the Doppler PSD corresponds to the Doppler frequency PDF imposed by the underlying scattering distribution [14]. To establish the relationship between the scattering distribution and the Doppler PDF, the important geometrical relationships are outlined first.

We recall that all multipath components arriving at the Rx with the same inclination angle to the mobile antenna velocity vector exhibit the same Doppler frequency shift. These directions define a circular cone with its apex at the mobile antenna position and the axis parallel to the velocity vector [15]. Fig. 1 illustrates the Doppler cone for a Doppler frequency f_* , with the coordinate system chosen such that the z -axis is aligned with the mobile antenna velocity vector.²

The figure also shows a unit sphere, over which the distribution of DoAs is defined. The points on the circular intersection of this sphere and the Doppler cone, indicated by the black dashed line, correspond to the unit DoA vectors associated with the same Doppler frequency shift, i.e.

$$f_* = f_m \cos \theta_* \quad (5)$$

where

- f_m maximum Doppler shift, i.e., $f_m = \|\mathbf{v}\|/\lambda$;
- θ_* angle between the DoA and the motion direction.

The area of the sphere within the Doppler cone (shown in red) corresponds to the directions for which the Doppler frequencies are higher than f_* , and the sphere area outside of the cone (shown in blue) corresponds to the lower Doppler frequencies.

Based on these observations, the Cumulative Distribution Function (CDF) of the Doppler frequency can be expressed as

$$F_{f_D}(f_*) = \int_{-\pi/2}^{\psi_*} \int_{-\pi}^{\pi} p_{\phi\psi}(\phi, \psi) d\phi d\psi \quad (6)$$

where

²This choice of the coordinate system yields no loss of generality, since the relative geometry is preserved.

ψ_* angle complementary to θ_* (Fig. 1).

By inserting (4) into (6) and applying [16, Eq. 3.338.4] to solve the inner integral in the azimuth angle ϕ , we obtain

$$F_{fD}(f_*) = \frac{\kappa}{2 \sinh \kappa} \int_{-\pi/2}^{\psi_*} I_0(a \cos \psi) e^{b \sin \psi} \cos \psi d\psi \quad (7)$$

where

$$a = \kappa \sqrt{\hat{k}_x^2 + \hat{k}_y^2} \quad (8)$$

$$b = \kappa \hat{k}_z \quad (9)$$

with $\hat{k}_{x/y/z}$ denoting the components of the mean DoA vector,

$$\mathbf{k}_\mu = (\cos \mu_\phi \cos \mu_\psi, \sin \mu_\phi \cos \mu_\psi, \sin \mu_\psi)^T \quad (10)$$

The Doppler PDF can be obtained as the derivative of (7) with respect to f_* . Applying the Leibnitz integral rule yields³

$$p_{fD}(f_*) = \frac{\kappa}{2 \sinh \kappa} I_0(a \cos \psi_*) e^{b \sin \psi_*} \cos \psi_* \frac{d\psi_*}{df_*} \quad (11)$$

From (5), ψ_* can be expressed as

$$\psi_* = \arcsin\left(\frac{f_*}{f_m}\right), \quad |f| \leq f_m \quad (12)$$

and we have

$$\frac{d\psi_*}{df_*} = \frac{1}{f_m \sqrt{1 - \left(\frac{f_*}{f_m}\right)^2}} \quad (13)$$

By replacing (13) in (11), recalling the complementarity of ψ_* and θ_* and using (5) to express $\cos \psi_*$ and $\sin \psi_*$ in terms of f_* , we obtain ($|f| \leq f_m$)

$$p_{fD}(f) = \frac{1}{2f_m} \frac{\kappa}{\sinh \kappa} I_0\left(a \sqrt{1 - \left(\frac{f}{f_m}\right)^2}\right) e^{b \frac{f}{f_m}} \quad (14)$$

where f is used instead of f_* to simplify the notation.

By noting that a in (8) is a function only of the component of the mean DoA vector perpendicular to the antenna motion direction, we can write

$$a = \kappa \sqrt{1 - (\hat{\mathbf{k}}_\mu^T \hat{\mathbf{v}})^2} \quad (15)$$

where

$\hat{\mathbf{v}}$ motion direction unit vector, i.e. $\hat{\mathbf{v}} = \mathbf{v}/\|\mathbf{v}\|$.

By inserting (15) and (9) in (14), the Doppler PDF for an arbitrary velocity vector can be finally written as

$$p_{fD}(f) = \frac{1}{2f_m} \frac{\kappa}{\sinh \kappa} e^{\kappa (\hat{\mathbf{k}}_\mu^T \hat{\mathbf{v}}) \frac{f}{f_m}} \times I_0\left(\kappa \sqrt{1 - (\hat{\mathbf{k}}_\mu^T \hat{\mathbf{v}})^2} \sqrt{1 - \left(\frac{f}{f_m}\right)^2}\right), \quad |f| \leq f_m \quad (16)$$

where

$I_0(\cdot)$ modified Bessel function (first kind, zeroth order).

³Only the upper limit of integration in (7) is a function of f_* , given by (12), while the integrand and the lower limit are invariant with respect to f_* .

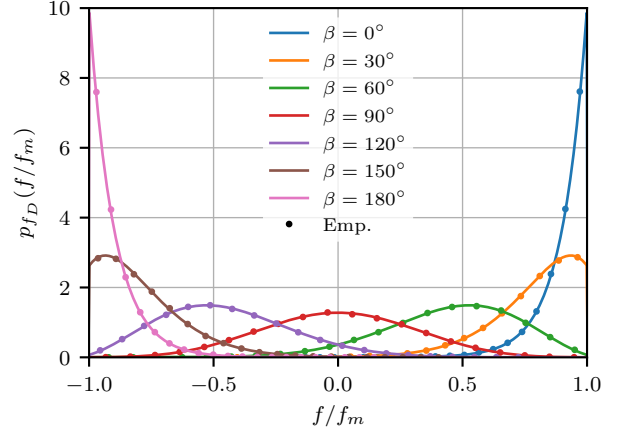


Fig. 2. Doppler PDF as a function of the angle β between the velocity vector and mean DoA ($\kappa = 10$); dots represent results obtained via simulation.

The Doppler spectrum depends on both mobile speed and motion direction. In contrast to the results for the 2D scattering [3], [5], the Doppler PDF in (16) is finite for $f = \pm f_m$, with

$$p_{fD}(\pm f_m) = \frac{1}{2f_m} \frac{\kappa}{\sinh \kappa} e^{\pm \kappa (\hat{\mathbf{k}}_\mu^T \hat{\mathbf{v}})} \quad (17)$$

For the special case of isotropic scattering ($\kappa = 0$), the Doppler PDF is uniform, i.e.

$$p_{fD}(f) = \frac{1}{2f_m}, \quad |f| \leq f_m \quad (18)$$

On the other hand, for $\kappa \rightarrow \infty$ the Doppler PDF becomes

$$p_{fD}(f) = \delta(f - f_\mu) \quad (19)$$

where

f_μ Doppler shift for the mean DoA direction, i.e.

$$f_\mu = f_m (\hat{\mathbf{k}}_\mu^T \hat{\mathbf{v}}) = f_m \cos \beta \quad (20)$$

β angle between the vectors \mathbf{k}_μ and $\hat{\mathbf{v}}$.

Therefore, scattering is deterministic in this case, with a single scatterer in the direction corresponding to the mean DoA.

IV. RESULTS ANALYSIS

In this section we employ the obtained analytical results to investigate the impact of vMF scattering parameters. To this end, the effect of the mean DoA direction and the concentration of scatterers around this direction is analyzed.

Fig. 2 shows the Doppler PDF, i.e., Doppler spectrum normalized to unit power, for different relative angles between the mobile antenna motion direction and the mean DoA. For motion perpendicular to the mean DoA ($\beta = 90^\circ$), the Doppler PDF is observed to be an even function. As the motion direction inclines towards the mean DoA ($\beta < 90^\circ$) or opposite to it ($\beta > 90^\circ$), the PDF becomes skewed towards the maximum or minimum Doppler frequency, respectively. For motion parallel to the mean DoA ($\beta = 0^\circ, 180^\circ$), the Doppler PDF exhibits an exponential behavior. This follows as the Bessel function term in (16) is equal to one in this case, and the exponential term governs the shape of the Doppler PDF.

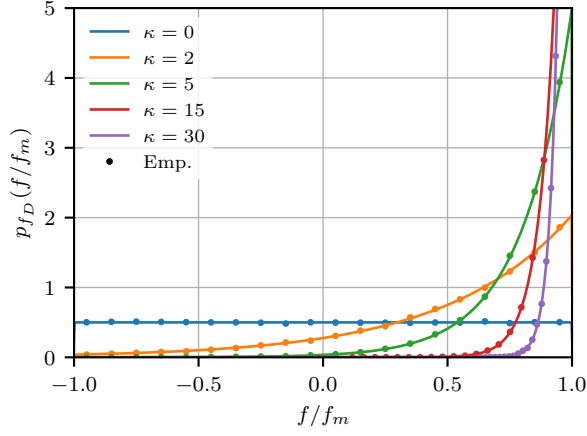
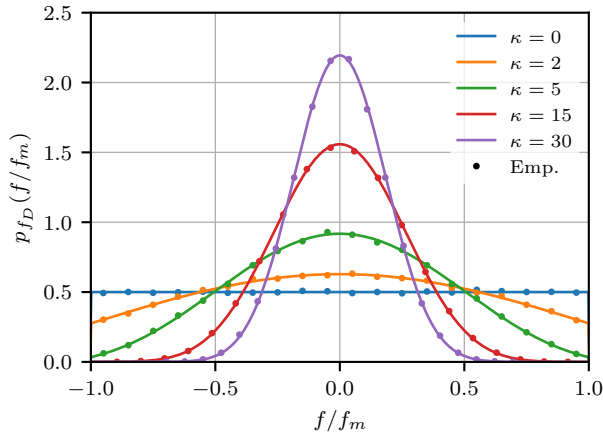
(a) $\beta = 0^\circ$.(b) $\beta = 90^\circ$.

Fig. 3. Doppler PDF as a function of the spread parameter κ for $\beta = 90^\circ$ and $\beta = 0^\circ$; dots represent results obtained via simulation.

Fig. 3 shows the Doppler PDF for different values of the angular spread parameter κ , in the case when the mean DoA is parallel (Fig. 3a) or perpendicular to the motion direction (Fig. 3b). For isotropic scattering ($\kappa = 0$), the Doppler PDF is seen to be uniform, regardless of the motion direction. The exponential trend of the Doppler PDF for $\beta = 0^\circ$ is evident from Fig. 3a, where more concentrated scattering (higher κ) yields a faster transition and a higher peak value at $f = f_m$, i.e., finite and given by (17).

As seen from Fig. 3b, the behavior of the Doppler PDF is different for $\beta = 90^\circ$. As scattering becomes more concentrated in this case, the shape of the Doppler PDF becomes similar to that of a zero-mean Gaussian distribution with increasingly smaller variance. This behavior is determined by the Bessel function in (16), as the exponential term becomes equal to one in this case. It should be pointed out that the Gaussian shape of the Doppler spectrum is reported for aeronautical channels, e.g., see [12, Ch. 3.3].

Figs. 2 and 3 also show empirical results obtained via Monte Carlo simulation, i.e., based on 10^5 randomly generated scatterers. As we observe, the empirical results exactly match the theoretical ones in all cases.

V. CONCLUSIONS

The vMF distribution is a widely adopted scattering model, particularly in multi-antenna systems performance studies where accurate spatial scattering distribution is of primary importance. However, second-order channel statistics associated with this scattering model are not yet fully investigated, with the corresponding Doppler characteristics receiving little or no attention in the existing literature.

To address this gap, in this work we derive a simple closed-form expression for Doppler power spectrum in vMF scattering channels. We use the obtained result to investigate the impact of the scattering parameters, i.e., the mean scattering direction and the degree of angular concentration. The Doppler spectrum is observed to exhibit Gaussian shape for mobile antenna motion perpendicular to the mean scattering direction, and an exponential one for the parallel motion.

REFERENCES

- [1] W. C. Jakes, *Microwave Mobile Communications*. New York, NY, USA: IEEE Press, 1974, ch. Ch. 1 Multipath Interference.
- [2] A. F. Molisch, *Wireless Communications*, 2nd ed. Chichester, UK: John Wiley & Sons, 2011.
- [3] R. H. Clarke, "A Statistical Theory of Mobile-Radio Reception," *Bell Syst. Tech. J.*, vol. 47, no. 6, pp. 957–1000, July 1968.
- [4] A. S. Akki, "Statistical Properties of Mobile-to-mobile Land Communication Channels," *IEEE Trans. Veh. Technol.*, vol. 43, no. 4, pp. 826–831, Nov. 1994.
- [5] A. Abdi, J. A. Barger, and M. Kaveh, "A Parametric Model for the Distribution of the Angle of Arrival and the Associated Correlation Function and Power Spectrum at the Mobile Station," *IEEE Trans. Veh. Technol.*, vol. 51, no. 3, pp. 425–434, May 2002.
- [6] T. Aulin, "A Modified Model for the Fading Signal at a Mobile Radio Channel," *IEEE Trans. Veh. Technol.*, vol. 28, no. 3, pp. 182–203, Aug. 1979.
- [7] J. D. Parsons and A. Turkmani, "Characterisation of Mobile Radio Signals: Model Description," *IEE Proc. 1 Commun., Speech Vis.*, vol. 138, no. 6, pp. 549–556, Dec. 1991.
- [8] K. Mammassis, R. W. Stewart, and J. S. Thompson, "Spatial Fading Correlation model using mixtures of Von Mises Fisher distributions," *IEEE Trans. Wireless Commun.*, vol. 8, no. 4, pp. 2046–2055, Apr. 2009.
- [9] K. Turbic, M. Kasparick, and S. Stanczak, "Correlation Properties in Channels with von Mises-Fisher Distribution of Scatterers," *IEEE Wireless Commun. Lett.*, 2024, Under revision for resubmission.
- [10] L. Zeng, X. Liao, Z. Ma, H. Jiang, and Z. Chen, "UAV-to-UAV MIMO Systems Under Multimodal Non-Isotropic Scattering: Geometrical Channel Modeling and Outage Performance Analysis," *IEEE Internet Things J.*, 2024, Early Access (April 30, 2024).
- [11] J. T. Y. Ho, "Generalized Doppler Power Spectrum for 3D Non-isotropic Scattering Environments," in *Proc. IEEE Global Telecommun. Conf. (GLOBECOM)*, St. Louis, MO, USA, Nov. 2005.
- [12] M. Pätzold, *Mobile Radio Channels*, 2nd ed. West Sussex, UK: John Wiley & Sons Ltd., 2012.
- [13] K. V. Mardia and P. E. Jupp, *Directional Statistics*. Chichester, UK: John Wiley & Sons, 2000.
- [14] A. Goldsmith, *Wireless Communications*. New York, NY, USA: Cambridge University Press, 2005.
- [15] R. Narasimhan and D. C. Cox, "A Generalized Doppler Power Spectrum for Wireless Environments," *IEEE Commun. Lett.*, vol. 3, no. 6, pp. 164–165, Jun. 1999.
- [16] I. S. Gradshteyn and J. M. Ryzhik, *Table of Integrals, Series, and Products*, 7th ed. San Diego, California, USA: Academic Press, 2007.